N92-24151

A Tone-Aided/Dual Vestigial Sideband (TA/DVSB) System for Mobile Satellite Channels

Gary J. Saulnier, Gilbert M. Millar and Anthony D. de Paolo
Electrical, Computer and Systems Engineering
Rensselaer Polytechnic Institute
Troy, New York 12180-3590
Tel:(518)276-2762
Fax:(518)276-6261

ABSTRACT

Tone-aided modulation is one way of combating the effects of multipath fading and Doppler frequency shifts. This paper discusses a new tone-aided modulation format for M-ary phase-shift keyed signals (MPSK). A spectral null for the placement of the tone is created in the center of the MPSK signal by translating the upper sideband upwards in frequency by one-half the null width and the lower sideband downwards in frequency by the same amount. The key element of the system is the algorithm for recombining the data sidebands in the receiver, a function that is performed by a specialized phase-locked loop (PLL). The system structure is discussed and simulation results showing the PLL acquisition performance are presented.

INTRODUCTION

Mobile-satellite channels are characterized as having Rician multipath fading and Doppler frequency shifts. Due to the narrowband nature of the channels and, in particular, the magnitude of the expected Doppler shifts with respect to the channel bandwidth, the receiver must perform some type of adaptation to the channel in order to maintain acceptable performance. One approach to performing this adaptation uses a tone contained within the signal to calibrate the receiver to the channel characteristics. Such tone-aided modulation has been shown to remove the irreducible error floor that is associated with many modulations in the Rician channel (Rafferty, 1987).

While a number of tone-aided modulation schemes have been proposed (Davarian, 1987, Simon, 1986, McGeehan, 1984) each has some drawback which has detracted from its usefulness. One problem common to all the tone-aided schemes is the undesirable bandwidth expansion of the signal necessary to accommodate the one or more tones. The TA/DVSB system discussed in this paper attempts to minimize the bandwidth expansion by using a single tone placed in a spectral null that is only as wide as is necessary to accommodate the Doppler spread. Results for a binary PSK TA/DVSB system have been reported earlier (Hladik, 1989) and this paper extends this work to MPSK.

As shown in Figure 1, the TA/DVSB signal consists of a tone inserted between the frequency-translated upper and lower vestigial sidebands of a phase modulated carrier. The modulator creates this signal by separating the sidebands and frequency translating the upper sideband upwards in frequency by f_t and the lower sideband downwards by the same amount. Although the TA/DVSB spectrum is similar to that of another tone-aided system, Transparent-Tone-In Band (TTIB) (McGeehan, 1984), the TA/DVSB demodulator uses a different algorithm for recombining the data sidebands. A major consequence of the TA/DVSB recombination algorithm is that

the vestigial sidebands can be kept as small as possible (ideally they would be zero), minimizing the required transmission bandwidth. The translation frequency, f_t, is selected to accommodate the expected Doppler spread while allowing for recovery of the tone in the receiver. Typically, f_t must equal twice the expected Doppler shift so that the pilot recovery filter can extract the tone without any data sideband energy.

MODULATOR

The TA/DVSB modulator accepts M-ary symbols and a produces root-Nyquist MPSK signal whose sidebands have been separated and frequency translated as shown in Figure 1. The tone is also inserted in the modulator. A number of approaches for generating the vestigial sidebands were considered, including Weaver's single sideband (SSB) modulator and the phase-shift SSB modulator (Carlson, 1975). However, a third approach in which SSB signals are directly synthesized was chosen.

Figure 2 is a block diagram of the MPSK TA/DVSB modulator. Consider the processing of the in-phase (I) data first. Impulses representing the I data are input into two transversal filters, one having an impulse response equal to the root-Nyquist pulse shape and a second having an impulse response equal to the Hilbert Transform of the root-Nyquist pulse shape. The outputs from these filters, then, are the pulse shaped I data, $d_I(t)$, and the Hilbert Transform of the I pulse-shaped data, $\hat{d}_I(t)$. These signals are then placed on a carrier of ω_t, where ω_t is the translation frequency, i.e $\omega_t=2\pi f_t$. The resulting signal is the I portion of the baseband TA/DVSB signal,

$$S_I(t)=d_I(t)\cos\omega_t t + \hat{d}_I(t)\sin\omega_t t. \quad (1)$$

The quadrature-phase (Q) data undergoes identical processing producing

$$S_Q(t)=d_Q(t)\cos\omega_t t + \hat{d}_Q(t)\sin\omega_t t. \quad (2)$$

$S_I(t)$ and $S_Q(t)$ are finally multiplied by quadrature sinusoids at the carrier frequency, ω_c, and summed to create the modulator output. When a DC component is added to $S_I(t)$, the tone will appear in the output. The composite output, then, is

$$\begin{aligned} S(t)=&[d_I(t)+\hat{d}_Q(t)]\cos[(\omega_c-\omega_t)t] \\ &+[-\hat{d}_I(t)+d_Q(t)]\sin[(\omega_c-\omega_t)t] \\ &+[d_I(t)-\hat{d}_Q(t)]\cos[(\omega_c+\omega_t)t] \quad (3) \\ &+[\hat{d}_I(t)+d_Q(t)]\sin[(\omega_c+\omega_t)t] \\ &+DC\cos(\omega_c t). \end{aligned}$$

Figure 3 is a transmit spectrum generated using the modulator of Figure 2. The shaping is 65% excess bandwidth root-Nyquist, ω_t is 480Hz and ω_c is 6kHz. The shaping filters use 10 samples per symbol and extend over 8 symbols.

DEMODULATOR

The demodulator consists of a pilot processor, sideband separation processors, a phase-locked loop (PLL) and pulse-shape matched filters. Figure 4 shows this structure.

Pilot Processor

Figure 5 is a block diagram of the pilot processor. The input to the pilot processor is the modulator output (3) after it has been passed through the channel which introduces additive white Gaussian noise (AWGN) along with multipath fading and Doppler frequency shift. The pilot processor assumes that both the tone and the data sidebands have undergone the same phase distortions in the channel and, consequently, uses the pilot as a coherent reference to remove these distortions.

The pilot processor first mixes the input signal to baseband I and Q signals using a local reference, ω_{LO}, which is approximately equal to ω_c.

Since the carrier of the received signal will be offset from ω_c due to Doppler frequency shifts and multipath fading, the I and Q signals will be on a carrier equal to the amount of this frequency offset and the pilot tone frequency will be equal to this offset frequency. Each signal then is broken into two paths, one which uses a lowpass filter to recover the pilot tone, I_P or Q_P, and a second which delays the corresponding I or Q signal by an amount equal to the delay of the lowpass filter.

The pilot tone components, I_P and Q_P, are then subtracted from the corresponding I and Q signals, effectively implementing highpass filters. I_P and Q_P are finally used as coherent references to remove the frequency offset from the I and Q signals. In the absence of noise the pilot processor outputs, I_O and Q_O, will equal the I and Q signals in the modulator as given by (1) and (2).

Sideband Separation Processor

The sideband separation processors act to isolate the upper and lower sidebands from each other, delivering each to the PLL. While this separation can be performed using lowpass and highpass filters if the signal is placed on a carrier, this type of bandpass processing is expensive in a DSP format. Consequently it was decided to perform the sideband separation at baseband using a Hilbert Transform filter. The resulting baseband SSB signals will be complex signals.

Figure 6 is a block diagram of the sideband separation processor. An input signal, x(t), is split into two paths, one which uses a transversal filter to perform a Hilbert Transform and a second which introduces a delay equal to the delay of the Hilbert Transform filter. The Hilbert Transform filter output, $\hat{x}(t)$ is used to create the two SSB signals. The upper sideband (USB) is

$$x_{USB}(t)=x(t) + j\hat{x}(t) \qquad (4a)$$

and the lower sideband (LSB) is

$$x_{LSB}(t)=x(t) - j\hat{x}(t). \qquad (4b)$$

Figure 7 shows recovered USB and LSB signals which have been placed on a carrier of 6kHz for display. The Hilbert Transform filter used was of 101st order.

Phase-Locked Loop

The PLL operates on the outputs of the sideband separation processors and locks a local oscillator to f_t, which is then used to recombine the data sidebands. It is important to note, however, that the PLL does not have to track any channel perturbations since the pilot processor removes these prior to the PLL. The output of the PLL is the recombined data sidebands which are then processed by filters that are matched to the root-Nyquist pulse shape.

As shown in Figure 8, there are four inputs to the PLL, the USB and LSB signals derived from each of the pilot processor outputs, I_O and Q_O. At the heart of the PLL is a voltage controlled oscillator (VCO) which generates a local approximation to ω_t which will be indicated as ω_r. The two VCO outputs are

$$r_1(t)=\exp[j(\omega_r t + \theta_r)] \text{ and} \qquad (5a)$$

$$r_2(t)=\exp[-j(\omega_r t + \theta_r + \pi/2)], \qquad (5b)$$

where θ_r is the phase of ω_r.

Consider the processing of the USB and LSB signals which originate from the I signal. These signals can be expressed as

$$USB(t)=[d_I(t)+j\hat{d}_I(t)]\exp[-j(\omega_t t+\theta_t)]$$

and (6a,b)

$$LSB(t)=[d_I(t)-j\hat{d}_I(t)]\exp[+j(\omega_t t+\theta_t)],$$

where the phase of ω_t is θ_t. USB(t) is multiplied by $r_1(t)$ while LSB(t) is multiplied by $r_2(t)$. The complex conjugate of the $LSB(t)r_2(t)$ product is then multiplied by the $USB(t)r_1(t)$ product to obtain the in-phase error signal

$$e_I(t)=[d_I^2(t)-\hat{d}_I^2(t)]\sin[2(\omega_t-\omega_r)t +2(\theta_t-\theta_r)]+2d_I\hat{d}_I\cos[2(\omega_t-\omega_r)t +2(\theta_t-\theta_r)]+\text{imaginary terms,} \quad (7a)$$

where the imaginary terms are not listed since they are discarded. Processing of the USB and LSB from the Q signal results in the error signal

$$e_Q(t)=[d_Q^2(t)-\hat{d}_Q^2(t)]\sin[2(\omega_t-\omega_r)t +2(\theta_t-\theta_r)]+2d_Q\hat{d}_Q\cos[2(\omega_t-\omega_r)t +2(\theta_t-\theta_r)]+\text{imaginary terms.} \quad (7b)$$

These error signals contain the desired $\sin[2(\omega_t-\omega_r)t-2(\theta_t-\theta_r)]$ term which, when minimized, would drive ω_r and ω_t to the same frequency and phase. The problem, however, is that this term is multiplied by a coefficient that is dependent on the data and its Hilbert Transform. In addition, there is a $\cos[2(\omega_t-\omega_r)t-2(\theta_t-\theta_r)]$ term which, if minimized, would drive the VCO to a quadrature lock.

Simulation of the PLL using either $e_I(t)$ or $e_Q(t)$ as the error signal indicated that the loop could not acquire lock. Actually, for small loop gains, the PLL would tend to maintain its initial phase value, indicating that $e_I(t)$ and $e_Q(t)$ have zero mean. A later analysis showed that the coefficients for both the sine and cosine terms are zero mean.

Through simulation it was determined that hardlimiting the error signal makes the PLL acquire and maintain phase lock. This hardlimiter is indicated in Figure 8, where the error signals from the I and Q channels, $e_I(t)$ and $e_Q(t)$ are first summed and then hardlimited before being sent to the VCO. As will be shown in the next section, this PLL has a considerable amount of self noise which restricts the maximum PLL bandwidth and thereby limits its acquisition performance.

Finally, examination of (7) indicates that the error signal will not suffer from self noise if the data signals, $d_I(t)$ and $d_Q(t)$, do not make any transitions, since the Hilbert Transform terms will all be zero. Consequently, transmitting the same data symbol several times as a preamble is viable approach for obtaining fast acquisition. This property will be demonstrated in the next section.

SIMULATION RESULTS

This section illustrates the performance of the PLL by showing a received eye diagram and a number of PLL acquisition curves. The channel was not included in these simulations and, consequently, the pilot processor was also omitted. The modulator output, at baseband, was fed directly to the sideband separation processors which, in turn, fed the PLL. 8-PSK signalling with root-Nyquist pulse shaping (65% excess bandwidth) was used in the simulations.

Figure 9 is a received eye diagram obtained after the PLL has locked. The loop gain for this diagram was 10^{-4}, a value that produces a tight lock point. This eye diagram was generated after the signal was match filtered. The inter-symbol interference evident in the eye diagram is most likely due to distortion of the low frequency components caused by the sideband separation operation in the modulator.

Figure 10 is a set of PLL acquisition curves for a random data input using loop gain as a parameter. The self noise caused by the presence of the Hilbert Transform components in the error signal is evident. Figure 11

is a set of PLL acquisition curves for a constant data symbol input, i.e. no data transitions. These acquisition curves are linear due to the hardlimiter in the error signal path. Clearly, fast acquisition of the f_t signal is possible with a preamble consisting of a constant data symbol.

CONCLUSIONS

This paper shows that the TA/DVSB system is a viable approach to tone-aided modulation. The baseband implementation of the modulator and demodulator is of relatively low complexity. For burst-mode communications, where fast acquistion of f_t is required, a preamble consisting of the same symbol repeated a number of times is required due to the self-noise of the PLL.

REFERENCES

1. **Carlson, A.B.** 1975. *Communication Systems*. McGraw-Hill.
2. **Davarian, F.** 1987. Mobile digital communications via tone calibration. *IEEE Transactions on Vehicular Technology*. VT-36, pp.55-62.
3. **Hladik, S.M., Saulnier, G.J. and Rafferty, W.** 1989. A tone-aided dual vestigial sideband system for digital communications on fading channels. IEEE Military Communications Conference. pp.709-714.
4. **McGeehan, J.P., Bateman, A.J.** 1984. Phase-locked transparent tone-in-band (TTIB):A new spectrum configuration particularly suited to the transmission of data over SSB mobile radio networks. *IEEE Transactions on Communications*. COM-32, pp.81-87.
5. **Rafferty, W., Anderson, J.B., Saulnier, G.J.**, and Holm, J.R. 1987 Measurements and a theoretical analysis of the TCT fading channel radio system. *IEEE Transactions on Communications*. COM-35, pp. 172-180.
6. **Simon, M.K.** 1986. Dual-pilot tone calibration technique. *IEEE Transactions on Vehicular Technology*. VT-35, pp.63-70.

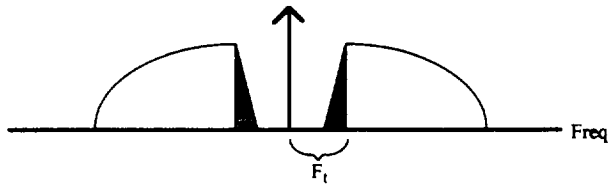

Fig. 1. TA/DVSB frequency spectrum

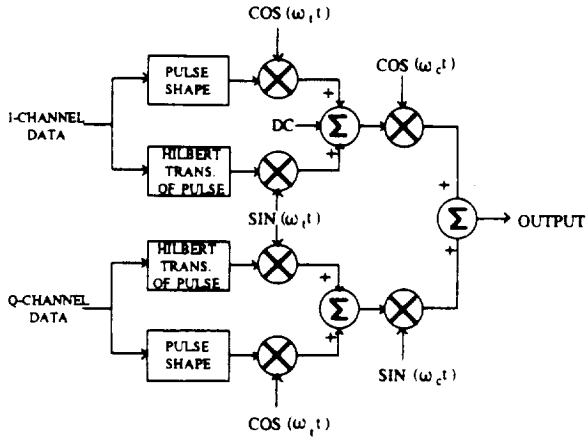

Fig. 2. TA/DVSB modulator

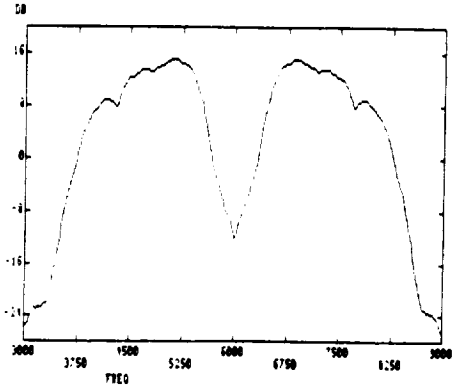

Fig. 3. Modulator output spectrum

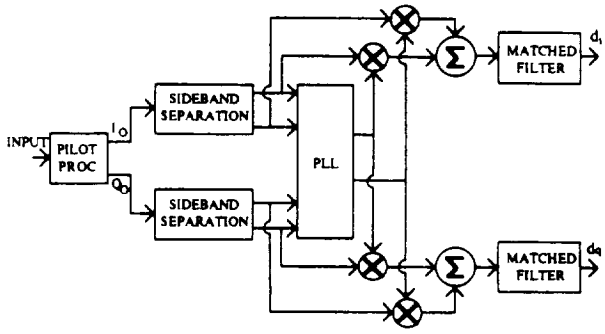

Fig. 4. TA/DVSB demodulator

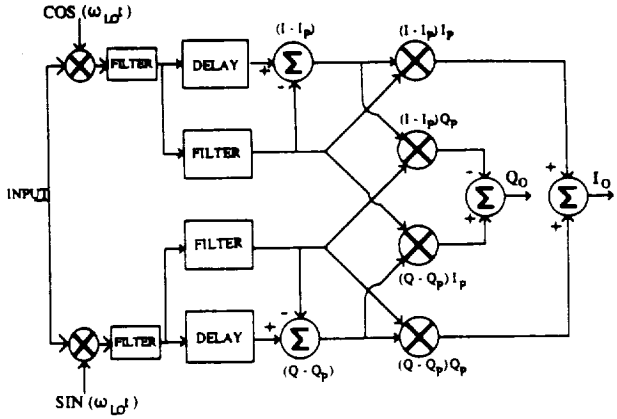

Fig. 5. Pilot processor

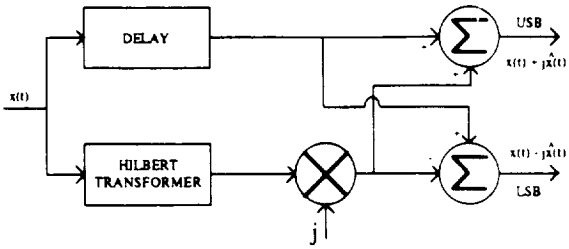

Fig. 6. Sideband separation processor

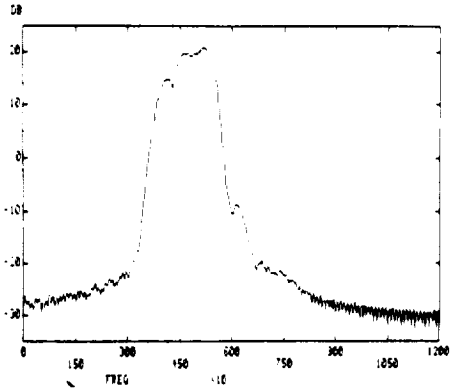

Fig. 7. Recovered sideband

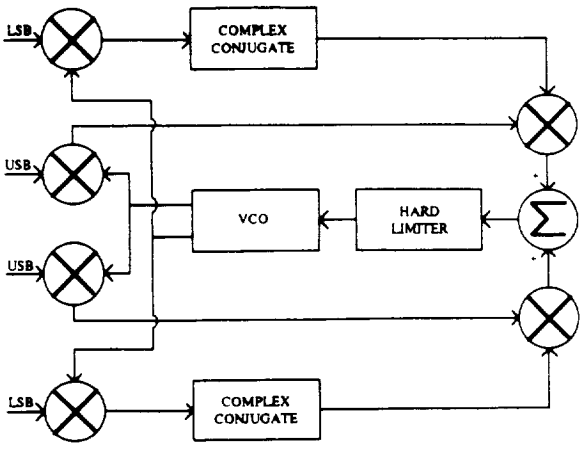

Fig. 8. TA/DVSB phase-locked loop

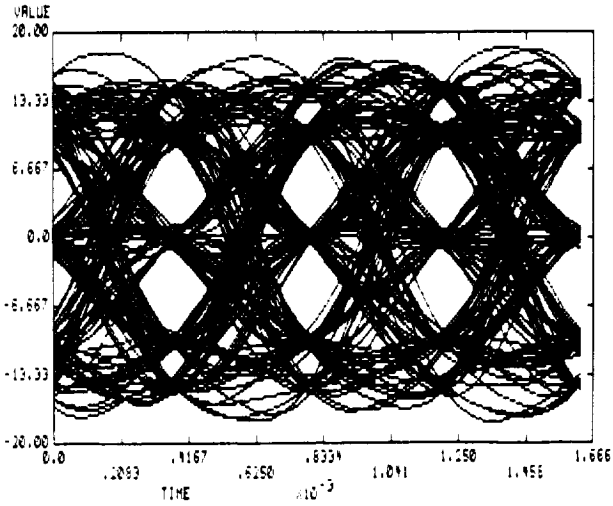

Fig. 9. Recovered eye diagram

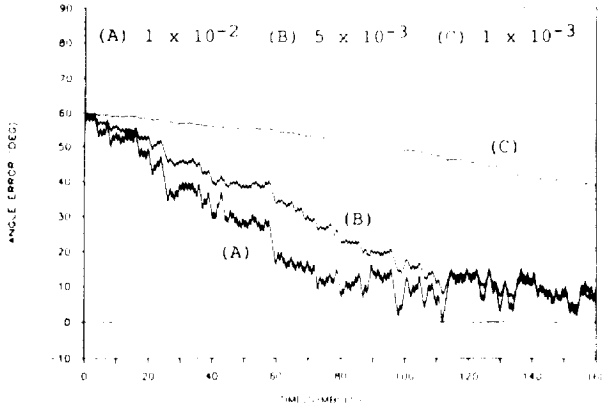

Fig. 10. Acquistion curves for random data

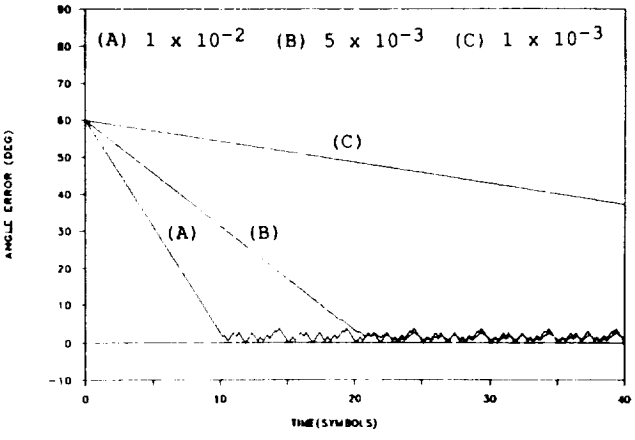

Fig. 11. Acquistion curves for no data transitions